Preliminary Results on Condition Monitoring of Fiber Ropes using Automatic Width and Discrete Length Measurements

Shaun Falconer[1], Andreas Gromsrud[2], Espen Oland[3] and Geir Grasmo[4]

[1,2,4] *University of Agder, Grimstad, Aust-Agder, 4879, Norway*
shaun.falconer@uia.no
andrg11@student.uia.no
geir.grasmo@uia.no

[3] *Teknova AS, Kristiansand, Vest-Agder, 4612, Norway*
espen.oland@teknova.no

ABSTRACT

As the offshore sector moves to deeper waters, fiber ropes have the potential to replace more traditional solutions such as steel wire ropes for deep sea lifting and heave-compensated operations. While steel wire ropes must account for their own weight when determining the maximum depth that a payload can be deployed, fiber ropes such as high modulus polyethylene (HMPE), are more buoyant than their steel counterparts, enabling payloads to be deployed at deeper depths using smaller cranes. For this reason, companies are actively developing fiber rope cranes to be used in industry. The inherent issue with these designs is monitoring the condition of the fiber rope due the multitude of damage mechanisms and condition indicators that exist, therefore determining the time to rupture remains an unsolved problem. To this end, this paper considers the use of computer vision to monitor the width at discrete length sections and use that as a potential condition indicator. Furthermore, the paper describes in detail how OpenCV is applied to detect the contour of the rope to find the width, how the experiment has been performed, as well as other practical experiences from testing a 28mm Dyneema® fiber rope. The experimental results show an exponential relationship between the applied tension and the reduction in width (which was reduced by more than 10% before rupture), and it is believed that if the width can be monitored at discrete sections along the rope over time, the width itself will prove to be a good condition indicator.

1. INTRODUCTION

Fiber ropes have been used in a offshore context for a variety of purposes including mooring and general sailing. While the use of fiber ropes in the marine sector is not a novel concept, the need to develop technology to adequately monitor their condition is of paramount importance and has substantial potential for progression. A particularly interesting alternative to steel wire ropes in offshore construction cranes that is gaining increasing popularity, is that of fiber ropes. There are already existing designs for fiber rope cranes by MacGregor, National Oilwell Varco and Rolls Royce. The greater buoyancy of HMPE fiber rope allows for smaller cranes to be used while potentially reaching water depths between 3000-4000m. Additionally this presents a saving in terms of mass and vessel deck space required for offshore operations when compared to steel wire rope designs. The inherent issue with this however is the effect of heave compensation on the fiber rope, which causes heat build up as it moves over the sheaves to keep the payload at the same depth relative to the ocean floor. This heat generation can lead to the ultimate degradation of the rope through creep, therefore a suitable means of monitoring the condition must be developed to judge the remaining useful life (RUL).

In terms of industry standards, it is recommended by (DNV-GL, 2005) that visual inspection of fiber rope is used to gauge its condition. While this is accepted practice there is still the distinct possibility for premature disposal of the rope due to conservative limits on their use. The natural extension of a visual inspection routine is the use of computer vision for monitoring purposes. Computer vision algorithms could be developed in order to automatically detect changes in the width and elongation of fiber rope and could serve as a valid condition indicator and lead to better understanding of the RUL of fiber rope used in offshore operations. Width and elongation measurements were chosen as the condition indicator based on recommendation from industry expert Nick O'Hear. Contributing factors towards inconsistent diameter measurement in fiber ropes include cut strands, compression damage,

Figure 1. Different kinds of rope damages. Cut strands (top left), compression damage (top right), inconsistent diameter (middle left) and pulled strands (middle right), heavy abrasion (bottom left) and melted fibers (bottom right). Reproduced with permission from Samson Rope Technologies.

pulled strands and heavy internal/external abrasion which can be seen in Figure 1. In a recent patent (Van Der Woude & Zijlmans, 2015) propose to correlate physical measurements related to rope diameter, rope shape, elongation, creep, bending, tension and temperature to specific positions along the rope to indication its current condition. Additionally another patent by (Ilaka & Zerza, 2014) makes use of a clamp and roller set up attached to springs to measure rope diameter. The lower set of spring rollers in this device have rotary axle where the measured diameter is transferred to a position sensor. As a result, cross sectional changes can be monitored to assess rope condition.

In general, condition monitoring of fiber ropes can be separated into two different types; embedded and non-embedded technologies. An example of embedded technology would be the inclusion of a foreign material into the rope. Using this approach it is possible to use magnetism, X-ray or terahertz analysis to assess the rope condition as was demonstrated in a patent by (Grabandt, Van Berkel, Oosterhuis, Mathew, & Akker, 2015).

However for the purposes of this article only non-embedded technologies will be considered. It is proposed that computer vision will automatically monitor the changing width and elongation through an algorithm formulated in OpenCV. In terms of previous work in this field, computer vision for condition monitoring has been researched using markings to detect the length of wire. An example of this is a patent by (Logan, Favrow, Haas, Stucky, & Baldwin, 2006) where markings on load bearing members in elevators are used for condition monitoring. The elongation between the markers is measured but there is no mention of the width. (Logan et al., 2006) also suggest the use of cameras as sensors for measuring the elongation between the markers. There has been little research into the use of monitoring the width of rope using computer vision.

This work will document the application and results of an OpenCV algorithm to detect the width and length changes in a 28mm Dyneema® fiber rope when subject to tension-tension testing. The conclusions from these tests will be discussed and potential steps for future research to progress condition monitoring of fiber ropes will be discussed.

2. COMPUTER VISION

Computer vision can be described as a computer understanding the world in the same way as humans do through vision. Through the use of digital images and videos, the digital signals can be processed through algorithms and interpreted as useful information. Computer vision contributes to a number of industries including manufacturing, medical diagnosis and robot guidance. An example of computer vision being used for condition monitoring purposes is in the agricultural industry. In their work, (Brosnan & Sun, 2002) used computer vision in the inspection of fruit and berries to classify their grade and quality.

The algorithm developed for this paper is based on color interpretation, therefore the main concepts are discussed in the following sections.

2.1. Software

The algorithm for width and elongation measurements was developed using OpenCV with Python chosen as the programming language. The versions used were OpenCV 3.2 and Python 3.6.

2.2. Color and Grayscale Representation

The outgoing digital signal from each pixel in an image is usually represented by 8-bit of information for each sensor in the pixel. If only one sensor is present in the pixel then the signal is represented by 256 different values specified on a scale where 0 is black and 255 is white. The computer interprets these different shades of gray as a designated numerical value for each pixel. In the case of color cameras, each pixel has three sensors with one to represent each of the primary colors (blue, green, red), known as "RGB representation". Incoming light to the camera is split into three different colors using optical filters and mirrors, where each of the primary colors will be represented by a scale with values from 0 to 255. This is equivalent to the possibility of 256^3 = 16,777,214 different colors that can be assigned to each pixel. Eq. (1) is the formula used by OpenCV when converting from color to grayscale:

$$Y = 0.299 \cdot Red + 0.587 \cdot Green + 0.114 \cdot Blue \quad (1)$$

where Y is the optimised grayscale value in relation to human perception of colors with regards to luminance (Moeslund, 2012). This will be used to turn the image of the fiber rope into grayscale representation before further processing.

2.3. Thresholding

Thresholding is used to separate background noise from the object of interest. In thresholding a value T between 0 and 255 is set, which will convert all pixel values under the threshold to 0 and those that are over to 255. This relationship is shown in Eq. (2) and Eq. (3):

$$\text{if } f(x,y) \leq T \text{ then } g(x,y) = 0 \tag{2}$$

$$\text{if } f(x,y) > T \text{ then } g(x,y) = 0 \tag{3}$$

where $f(x,y)$ and $g(x,y)$ are a specific pixel on an image before and after the thresholding operation respectively.

2.4. Hue, Saturation, Value (HSV)

Hue, Saturation, Value (HSV) is another method of representing colors in an image. Hue is the pure color represented by the dominant wavelength in the perceived light with a given value between 0 and 360 degrees, for example red, green and blue all have Hue values of 0, 120 and 240 degrees respectively. The Saturation and Value parameters represent the brightness and darkness of the colors used respectively, both of which can be denoted by a value between 0 and 255. HSV representation makes focusing on a specific color (i.e the color of the fiber rope) easier. As a default, OpenCV makes use of Blue, Green, Red (BGR) representation and must be converted to HSV representation. Conversion from RGB to HSV is performed by Eqs. (4), (5) and (6).

$$V = max(R,G,B) \tag{4}$$

$$S = \begin{cases} \frac{V - min(R,G,B)}{V} & \text{if } V \neq 0 \\ 0 & \text{otherwise} \end{cases} \tag{5}$$

$$H = \begin{cases} 60(G-B)/(V - min(R,G,B)) & \text{if } V = R \\ 120 + 60(B-R)/(V - min(R,G,B)) & \text{if } V = G \\ 240 + 60(R-G)/(V - min(R,G,B)) & \text{if } V = B \end{cases} \tag{6}$$

2.5. Border Method

In order to follow the outline of the fiber rope in the image, a border following algorithm is employed. OpenCV makes use of a contour finding method specified in work by (Suzuki & Abe, 1985), where a raster scan is applied to an input binary image. Essentially the algorithm follows pixels of the same intensity or color to find the contour of the fiber rope in the image.

Figure 2. Example of splice and eyelet at the end of a fiber rope speicmen.

2.6. Green's Theorem

Green's Theorem is applied in OpenCV to the find the moment of the enclosed area made by the contour. It describes the relation between the line integral around the closed curve C, and the double integral over the plane D which C has enclosed. If L and M have continuous first order partial derivatives on D and the path of integration is anticlockwise, then this can be represented as the mathematical expression shown in Eq. (7):

$$\oint_C (Ldx + Mdy) = \int\int_D (\frac{\partial M}{\partial x} - \frac{\partial L}{\partial y})dxdy. \tag{7}$$

3. EXPERIMENTAL SET-UP

The experiment consisted of multiple tension-tension tests on different HMPE fiber rope specimens. The tests were recorded and the video data was analysed using the OpenCV algorithm to detect width and length changes in the fiber rope specimens.

3.1. Equipment

The tension-tension testing was performed using a Wolport tensioner machine, which is capable of delivering a maximum load of 1000 kN. The fiber rope was secured into the machine using two 25 ton rated shackles attached to eyelets located at either end of the rope.

A 28mm Dyneema® fiber rope consisting of 12 strands each with 14 yarns was used. Eyelets for securing the rope into the tensioner were made through splicing performed in house at the University of Agder. The splice chosen was a modified version of the Tuck-Bury eye splice in order to make the rope specimen short enough to fit into the tensioner. It is worth note that if this type of splicing is performed correctly, the areas were the unspliced rope meets the spliced portion will experience a 5-15% reduction in strength. As this is a modified version of the splice, it is expected that this strength reduction will be at least 15% or higher in this splice transition zone. An example of the splice is shown in Figure 2.

The area where the width and length measurements will take place is the portion of the rope between both splice transition

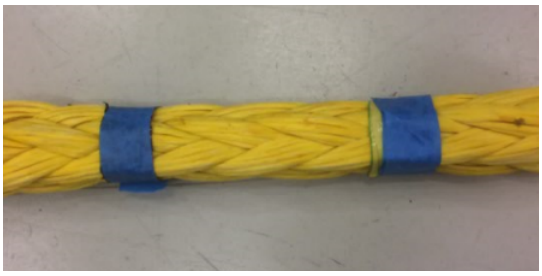

Figure 3. The area where width and length measurements were taken

Figure 4. Experimental set up. Here a fiber rope is secured into the tensioner.

zones highlighted in Figure 3. Blue markers are placed on this portion at roughly 100 mm apart for purposes of detecting length measurement in the OpenCV algorithm. Creep is a behaviour that occurs locally, therefore discrete measurements at different portions of the rope will be of interest.

The experiments were recorded using a Logitech C922 1080p web camera with a 1920x1080 resolution. Additionally the camera was full HD and recorded at 30 frames per second (fps). The camera was mounted so that it focused on the area of interest where measurement occurred. This video was then analyzed by the OpenCV algorithm.

A white backdrop was erected behind the tensioner rope in order to distinguish the colors of the rope and markers from background interference. The experimental set up is shown in Figure 4.

3.2. OpenCV Algorithm

3.2.1. Length Measurements

The markers were applied to the rope in the area to be tracked by the OpenCV algorithm. Blue was chosen as it contrasts the colors of the yellow rope and white background. The algorithm was programmed to measure the distance between these two markers.

To detect the blue markers every frame of the video is converted from RGB to HSV colour representation. The formula for the transformation process for each pixel is highlighted by Eqs (4), (5) and (6).

Once converted, a suitable search band has to be adjusted for the algorithm to detect the color blue. OpenCV uses a slightly different scale for the Hue portion of HSV representation as previously highlighted. OpenCV uses a scale of 0 to 179 for Hue, with blue to be equivalent to 120 in this range. Therefore the search band values (including Saturation and Value) are set with a lower band [90, 50, 50] and an upper band [150, 255, 255].

The contour is then detected around the marker sections using the border method in the black and white binary image. In order to avoid noise from smaller contours on the edge of the markers, a threshold is applied so that only the large blue areas in the range are detected. The area of interest in the rope along with the binary image after this process is shown in Figure 5.

Figure 5. Area with markers (left) and the binary image after HSV conversion and thresholding (right).

The image detected essentially works as a coordinate system. The centre point of both markers are found and given as points (x_1, y_1) and (x_2, y_2) for points 1 and 2 respectively. The distance between these points is used for the length measurements, which are highlighted in Figure 6.

3.2.2. Width Measurements

The width measurements took place in the area between the two markers. Three separate width readings were taken from this area and were denoted as regions of interest (ROI).

Figure 6. Measurement area with mid points of markers. The distance between these points are used for length measurements.

Figure 7. Areas with markers (left) and the binary image after HSV conversion and thresholding (right).

The same conversion from RGB to HSV conversation occurs, however in this instance the color of the rope is used. As the rope is yellow the search bands for HSV thresholding are set as a lower band [0, 50, 50] and [50, 255, 255]. The measurement area in the rope along with the binary image after this process is shown in Figure 7.

The contour is then found through the border method used for the length calculation. The green contour is then applied to the white portions of the binary image. Each pixel in the contour around the rope has an assigned coordinate. For each frame, the coordinates of each point in the contour are stored in two separate arrays for the left and right sides of the rope. This is performed for all three ROIs. The distance between each point on the left and each point on the right is calculated and the shortest distance is returned. This shortest distance represents the smallest width recorded in each frame and is show as a red line in Figure 8.

3.3. Method

Three different tests on separate rope specimens were performed with width and length measurements taken in the area between the markers applied to the rope. For all experiments

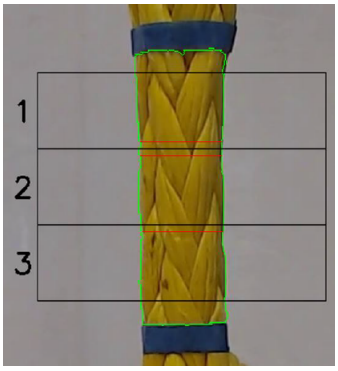

Figure 8. Measurement area with the three separate ROIs highlighted. The red line in each section denotes the shortest width measured during each frame.

the markers were applied at approximately 100mm apart. The common aim in each test was to stretch the rope in the tensioner until failure. Differences in terms of the markers used and loads applied are detailed in the following sections.

Experiment 1: A permanent marker pen is used to draw markers on the rope to be evaluated by the OpenCV algorithm. There was a pre-load phase were the tensioner holds the rope at 0.4kN and was steadily increased until 338.8kN before stopping the test.

Experiment 2: Blue markers were used for length measurements and to denote the area for the ROIs for width measurements. There was a pre-load phase were the tensioner holds the rope at 0.4kN and was steadily increased until 310kN before stopping the test.

Experiment 3: Blue markers were used for length measurements and to denote the area for the ROIs for width measurements. There was pre-load phase were the tensioner holds the rope at 1.5kN and was steadily increased until 290kN before stopping the test.

4. RESULTS

Three different experiments were performed using the described setup. In the following results, a moving average filter with window-size 50 has been used to smooth the width measurements, while the length measurement is smoothed using a filter with window size of 200.

In the first experiment the load was applied linearly from a pre-tension up to 338kN from where the rope ruptured in the splice above the region of interest. Figure 9 shows the experimental results, where it is evident that the width of the rope goes from 25.6mm down to 22.9mm at 150 seconds.

Table 1. Comparison of results.

Time	Exp 1	Exp 2	Exp 3
Load at rupture	338kN	310kN	295kN
Width reduction	10.5%	13.6%	11.2%
Length increase	N/A	N/A	1.9%

In the second experiment, the load is applied over a shorter time (100 seconds). Figure 10 shows the experimental results, where the width goes from 26.5mm down to 22.9mm right before rupture (from 140 seconds the width decreases linearly, which might be the initial stage of rupture). Pay special attention to the exponential shape of the reduction in width, which become apparent from this experiment. Going back to Figure 1, the same exponential relationship can be observed, but with a much larger time-constant.

While the intention for the two first experiments was to also measure the length using external markers, this proved to be somewhat more challenging than anticipated as the marker moved relative to the rope during the experiments. In the third experiment, this issue was remedied and these results therefore also contain the increase in length during the experiment. Further, the load is here increased in a step-wise manner up to 295kN, instead of linear increase, and over a much longer time. Figure 11 shows the applied load, the width of the rope together with the increase in length at the region of interest. In this experiment, the width goes from 25.8mm to 22.9mm, while the discrete length increases from 100mm to 101.9mm right before rupture. The increase in length is measured by fixing two markers placed 100mm from each-other. This means that the discrete length increases by 1.9%.

Table 1 shows a summary of the three experiments where it can be observed that the width of the rope decreases in the range of 10.5 - 13.6% before rupture, while the length in the third scenario increases by 1.9%. It is evident that the width and length of the rope changes during use, and as such can be good condition indicators. All three test-samples ruptured at 22.9mm, such that by monitoring the width and defining a minimum value might serve as a way forward. The differences in width reduction from the three experiments are due to sensor-noise and the fact that ropes are slightly different based on tension, temperature, construction, etc. This means that it is the change in diameter that should serve as a condition indicator, and not an absolute value based on the defined diameter of the rope.

5. DISCUSSION

In all three experiments there was an exponential decrease in the width measured as each load was increased. It is also worth note that the separate fiber rope specimens used all ruptured at a width of 22.9mm. Additionally the width measurements across all three experiments vary as there are different

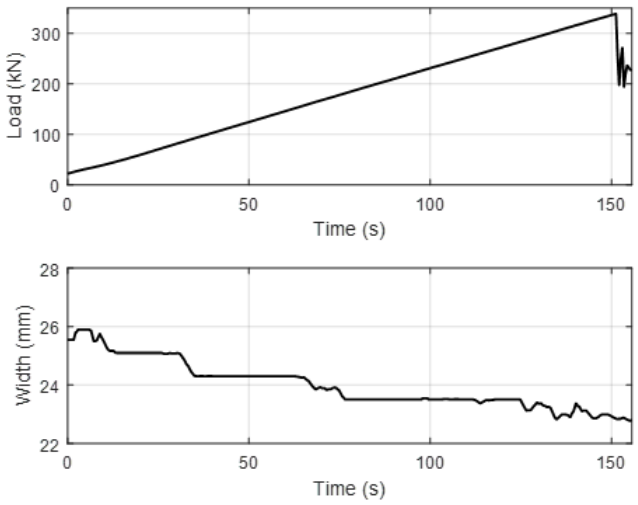

Figure 9. The first experiment where the load was increased linearly until rupture.

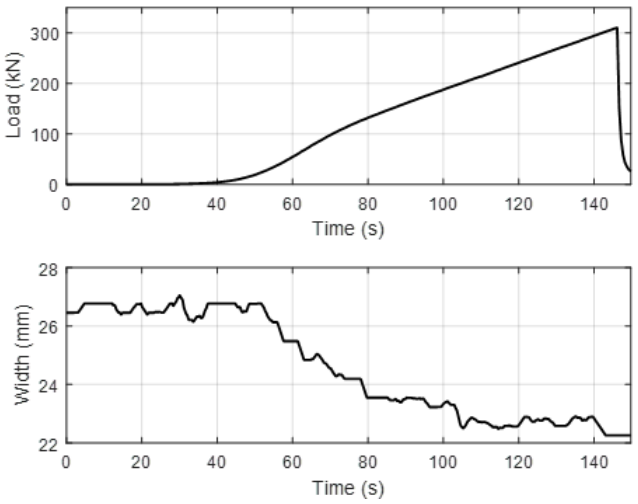

Figure 10. The second experiment where the load was applied (almost) linearly with a shorter duration than the first experiment.

starting widths from slight differences in each rope preparation routine. When each fiber rope specimen is prepared, a splicing process takes place and no two routines will be exactly the same, causing discrepancy in the measurements between each test. The ruptures that occurred during testing all came at the splice due to the reduction of the strength in this portion of the rope. In addition to this, as creep is a local phenomenon and will not act the same across the whole length of the rope contributing to varying results. The results do indicate that computer vision is a valid method of tracking the width of fiber rope during tension-tension tests. However in terms of length measurements a new method of attaching markers to the rope has to be found as the previous method led to invalid results from the first two experiments. The

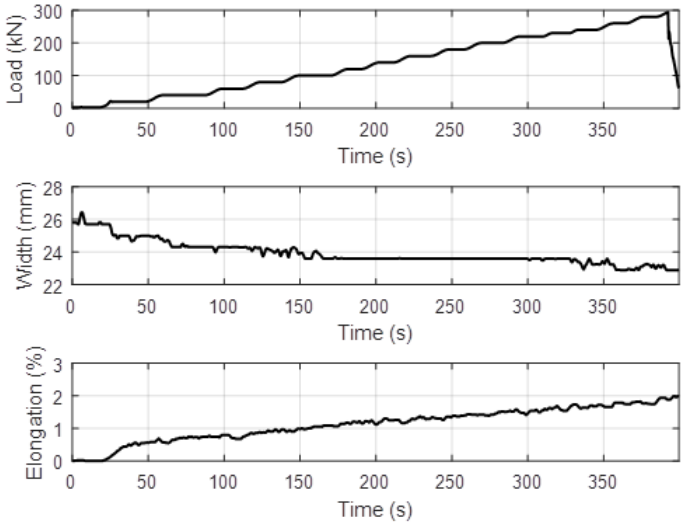

Figure 11. The third experiment with a step-wise load curve and a longer time-period.

length measurements from the third experiment indicate that it is possible to monitor the length but an improved method is required. Finally the overall results from the tension-tension tests conducted cannot be directly compared to the behavior of rope under long term creep at lower magnitude loads, however it has been demonstrated that changes in width measurements are detectable by applying this method and could be monitored over a longer period of time.

6. CONCLUSION

The overall results indicate that it is possible to monitor the width and length measurements of a fiber rope under tension-tension testing. They also indicate that there is potential in using these measurements as condition indicators to evaluate the state of a fiber rope. However, the application that is of most concern is the effect of heave compensation on fiber rope. In the future, it is proposed that this technology is applied to fiber rope undergoing a cyclic-bend-over-sheave (CBOS) regime to simulate the effects of offshore lifting operations. There is also the possibility that computer vision could be extended to monitor the rope for other damage such as cut and pulled strands affecting the outer geometry. Additionally, it is desirable to combine this with other technologies such as thermography, CT scanning and embedded conductive threads in the rope to monitor the condition of the rope and improve estimates of RUL by considering other damage mechanisms. It is hoped that with this potential combined technology approach, it will be used to log the conditions experienced by the fiber rope during offshore operations, of which width and elongation measurements detected by computer vision will form a constituent part.

ACKNOWLEDGMENT

The research presented in this paper has received funding from the Norwegian Research Council, SFI Offshore Mechatronics, project number 237896. The authors would also like to extend a special thanks to Cecilie Ødegård for her assistance during the experiments performed through this work.

REFERENCES

Brosnan, T., & Sun, D. W. (2002). Inspection and grading of agricultural and food products by computer vision systems - A review. *Computers and Electronics in Agriculture*, *36*(2-3), 193–213. doi: 10.1016/S0168-1699(02)00101-1

DNV-GL. (2005). Damage Assessment of Fibre Ropes for Offshore Mooring.

Grabandt, O., Van Berkel, B., Oosterhuis, F., Mathew, T., & Akker, P. G. (2015). *Method for non-destructive testing of synthetic ropes and rope suitable for use therein.*

Ilaka, M., & Zerza, H. (2014). *Patent US 2014/0027401 A1: Apparatus for recognising the discard state of a high-strength fiber rope in use in lifting gear.* doi: 10.1016/j.micromeso.2003.09.025

Logan, D. E., Favrow, L. H., Haas, R. J., Stucky, P. A., & Baldwin, N. R. (2006). *Patent US 7117981B2: Load Bearing member for use in an elevator system having external markings for indicating a condition of the assembly.*

Moeslund, T. B. (2012). *Introduction to video and image processing: Building real systems and applications*. Springer Science & Business Media.

Suzuki, S., & Abe, K. (1985). Topological structural analysis of digitized binary images by border following. *Computer Vision, Graphics and Image Processing*, *30*(1), 32–46. doi: 10.1016/0734-189X(85)90016-7

Van Der Woude, F., & Zijlmans, J. (2015). *Patent WO 2015160254 A1: Real-time rope monitoring.*